In Vivo Requirement of Protein Prenylation for Maintenance of Retinal Cytoarchitecture and Photoreceptor Structure

Steven J. Pittler,* Steven J. Fliesler,‡ Patricia L. Fisher,§ R. Kennedy Keller,‖ and Laurence M. Rapp§

*Departments of Biochemistry and Molecular Biology and of Ophthalmology, College of Medicine, University of South Alabama, Mobile, Alabama 36688-0002; ‡Anheuser-Busch Eye Institute and Program in Cell and Molecular Biology, Saint Louis University Health Sciences Center, St. Louis, Missouri 63104; §Cullen Eye Institute, Department of Ophthalmology, Baylor College of Medicine, Houston, Texas 77030; ‖Department of Biochemistry and Molecular Biology, University of South Florida, College of Medicine, Tampa, Florida 33612.

Abstract. Recent studies have demonstrated that inhibition of mevalonate synthesis in cultured cells leads to altered cell morphology due to inhibition of protein prenylation. To investigate the effects in vivo of mevalonate deprivation in nondividing, terminally differentiated neural cells, we have analyzed the effects on retinal tissue of intravitreal injection of lovastatin, a potent inhibitor of the mevalonate-producing enzyme, HMG-CoA reductase. A single injection of lovastatin (0.25 μmol) produced profound dysplastic-like changes in adult rat retinas primarily involving the photoreceptor layer. Within 2 d after injection, photoreceptor nuclei migrated in a circular pattern resulting in the formation of rosette-like structures by 4 d. Also during this period, photoreceptor inner and outer segment degeneration was evident. By 21 d, intact photoreceptor nuclei with remnants of inner and outer segments were dispersed throughout all retinal layers. To investigate the biochemical specificity of the lovastatin-induced alterations, and to distinguish the relative importance of the various branches of the mevalonate pathway, the incorporation of [^{3}H]acetate into retinal lipids was examined in the presence and absence of metabolic inhibitors. HPLC analysis of lovastatin-treated retinas revealed a dramatic reduction in the incorporation of intravitreally injected [^{3}H]acetate into nonsaponifiable lipids, compared with controls. In contrast, intravitreal injection of NB-598, a specific inhibitor of squalene epoxidase, eliminated the conversion of newly synthesized squalene to sterols without obvious pathology. Hence, involvement of the sterol branch of isoprenoid metabolism in the lovastatin-induced morphologic disruption was obviated. Intravitreal injection of 0.27 μmol of *N*-acetyl-*S-trans,trans*-farnesyl-L-cysteine (AFC), an inhibitor of carboxyl methyltransferase activity and prenylated protein function, produced morphologic changes that were virtually indistinguishable from those induced with lovastatin. These results implicate a defect in protein prenylation in the lovastatin-induced retinal degeneration, and suggest the presence of a dynamic pathway in the retina that requires isoprenylated proteins to maintain retinal cytoarchitecture.

INHIBITION of mevalonate biosynthesis with 3β-hydroxy-3-methylglutaryl-coenzyme A (HMG-CoA)[1] reductase inhibitors (e.g., lovastatin) prevents the synthesis of sterols, dolichols, ubiquinone, isopentenyl modified tRNA, heme a, and the prenylation of cellular proteins such as the *ras* superfamily small GTP-binding proteins (Maltese, 1990; Schroepfer, 1981; Sinensky and Lutz, 1992; see Fig. 1). Treatment of cultured cells with lovastatin produces growth arrest, cell rounding, and an aberrant refractile morphology (for reviews see Hall, 1993; Goldstein and Brown, 1990). Recent data have suggested a role for the apparently ubiquitous *rho* class of small GTP-binding proteins in the modulation of cytoskeletal architecture in cultured mammalian cells (for review see Nobes and Hall, 1994). The first compelling evidence for the function of *rho* proteins was obtained by direct microinjection of constitutively active *rho*A protein into mouse fibroblasts (Paterson et al., 1990), causing cell rounding that was attributed to a primary effect on microfilaments. Disruption of intermediate filaments appeared to occur as a secondary effect of microfilament dissolution, while microtubules appeared unaffected. Studies done with a human renal carcinoma cell line provided independent confirmation that microfilament dissolution and changes in cell shape

Please address all correspondence to S. J. Pittler, Department of Biochemistry and Molecular Biology, College of Medicine, University of South Alabama, Medical Sciences Building, Room 2199, Mobile, AL 36688-0002. Tel.: (334) 460-6861. Fax: (334) 460-7134.

1. *Abbreviations used in this paper*: AFC, *N*-acetyl-*S-trans,trans*-farnesyl-L-cysteine; HMG CoA, 3β-hydroxy-3-methylglutaryl-coenzyme A; inl, inner nuclear layer; onl, outer nuclear layer; olm, outer limiting membrane; ris, rod inner segment; ros, rod outer segment; rpe, retinal pigment epithelium; gcl, ganglion cell layer.

occur upon blockage of protein prenylation (Fenton et al., 1992). Both *rho* and *rac* are prenylated at their COOH-termini with a geranylgeranyl isoprenoid. In mouse fibroblasts, *rho*A was shown to be required to induce focal adhesions (Ridley and Hall, 1992), whereas *rac*1 was necessary for membrane ruffling to occur (Ridley et al., 1992). *Rho* and *rac* were also essential to initiate de novo actin polymerization and for entrapment of released cortical filaments, respectively, during activation of rat peritoneal mast cells (Norman et al., 1994). Inhibition of *rho*A in neuronal cells by ADP ribosylation led to a loss of actomyosin contractility and promotion of neurite outgrowth (Jalink et al., 1994). Thus, at least two members of the *rho* class of *ras*-like proteins regulate specific aspects of cytoskeletal structure and function.

In the eye, intravitreal injection of [^{3}H]mevalonate revealed the prenylation of several retina proteins ranging in size from 8–100 kD (Anant et al., 1992). These proteins have been identified as rod cell cGMP phosphodiesterase α and β subunits (Anant et al., 1992; Qin et al., 1992), rod cell transducin γ subunit (Fukada et al., 1990; Pérez-Sala et al., 1991), rhodopsin kinase (Inglese et al., 1992) and at least three proteins in the 20–30-kD range, which have not been characterized rigorously. Based on their size, relative abundance, isoprenoid modification, methylation, and GTP binding (Pérez-Sala et al., 1991), the 20–30-kD proteins are likely to be members of the *ras* superfamily (for review see Hall, 1993). In a preliminary report, we previously showed that intravitreal injection of lovastatin into adult rat eyes profoundly disrupts retinal cell morphology (Pittler et al., 1992). Here, we describe in detail the morphological manifestations of this effect, and provide specific evidence that implicates disruption of protein prenylation, rather than other branchpoints of the isoprenoid metabolic pathway.

Materials and Methods

Adult female Long-Evans pigmented rats (200–250 g) (Harlan Sprague-Dawley, Indianapolis, IN, or Charles River Laboratories, Wilmington, MA) were maintained for at least one week on cyclic lighting (12 h light, 12 h dark) before use. All procedures involving animals conformed to the Association For Research in Vision and Ophthalmology, Committee on Animals in Research (Bethesda, MD; Statement for the Use of Animals in Ophthalmic and Vision Research, 1990) and the NIH Guide for the Care and Use of Laboratory Animals. [^{3}H]Acetate (Na salt, 27 Ci/mmol) was obtained from ICN Radiochemicals (Irvine, CA). ^{14}C-labeled cholesterol and squalene were obtained from American Radiolabeled Chemicals (St. Louis, MO). Lovastatin (a generous gift of Dr. A. Alberts, Merck Sharpe & Dohme, Rahway, NJ) was converted to the sodium salt (Kita et al., 1980) and stored lyophilized at −20°C. Just before use the drug was dissolved in 10 mM Tris, pH 7.4 (stock concentration, 20 mg/ml). NB-598 (a generous gift of Dr. M. Horie, Banyu Pharmaceutical Co., Ltd., Tokyo, Japan) was dissolved in Me_2SO (stock concentration, 10 mg/ml) before use. *N*-acetyl-*S*-*trans*,*trans*-farnesyl-L-cysteine (AFC; Biomol, Inc., Plymouth Meeting, PA) was dissolved in Me_2SO at a concentration of 30 mg/ml. All organic solvents were obtained from Burdick & Jackson (Muskegon, MI). Unless otherwise specified, all other analytical reagents and biochemicals were obtained from Sigma Chem. Co. (St. Louis, MO).

Intravitreal Injections

Intravitreal injections were performed as previously described (Pittler et al., 1992; Fliesler et al., 1993). For evaluation of the persistence of the effects of lovastatin or NB-598, one eye of each animal (three animals per group) was injected with either lovastatin (0.25 μmol in 5 μl Tris-HCl, pH 7.4) or NB-598 (50 μg in 5 μl Me_2SO); the contralateral eye received 5 μl of Me_2SO alone (control). Animals were injected 1, 3, or 7 d later in both eyes with [^{3}H]acetate (0.20–0.25 mCi/eye, in 5 μl PBS); after allowing 6 h for uptake and metabolism of the radiolabeled precursor, animals were enucleated, and the neural retinas were isolated.

Extraction and Analysis of Retina Nonsaponifiable Lipids

The procedures employed for the saponification, extraction, and analysis of retinal nonsaponifiable lipids were performed as previously described (Keller et al., 1988; Fliesler et al., 1993). The lower limit of detection was ~10 pmol for cholesterol and ~1 pmol for squalene. The elution positions for mass and radioactivity were calibrated using cholesterol and squalene standards. Since the extinction coefficient for squalene at 214 nm is ~10-fold greater than that of cholesterol, the relative integrated areas or heights of the *uv* peaks do not correspond directly to the amounts of cholesterol and squalene mass represented in the chromatograms. Absolute retention times for cholesterol and other isoprenoid components varied from day to day, due to changes in ambient room temperature. Authentic ^{14}C-labeled standards of cholesterol and squalene were employed before and after each set of HPLC analyses to verify and calibrate retention times.

Light and Electron Microscopy

At postinjection intervals ranging from 1 to 21 d, animals were given an overdose of sodium pentobarbital and both eyes were enucleated. The dissection and fixation protocols used in this study have been previously reported (Rapp and Smith, 1992). Briefly, after enucleation, whole eyes were immersed in a solution of 2.5% glutaraldehyde and 1% paraformaldehyde buffered with 0.125 M sodium cacodylate, pH 7.35. After 15 min the anterior segment was removed and the peripheral one-third of the nasal eyecup was trimmed off by making a cut in the vertical plane of the eye. The remaining tissue was fixed overnight at 4°C and post-fixed the next day in buffered 1% osmium tetroxide. This was followed by dehydration in graded ethanols and embedment in an Embed® 812-Araldite 502 plastic mixture (Electron Microscopy Sciences, Fort Washington, PA). Sections for light microscopy were cut at 0.5 μm and stained with 1% Toluidine Blue. For electron microscopy, 80–90-nm sections were cut from the same blocks, stained with 5% uranyl acetate and 2% lead citrate, and examined with a JEOL 100CX electron microscope.

Results

Intravitreal Lovastatin Induces Temporally Distinct Changes in Retinal Morphology

While numerous studies have analyzed the effects of lovastatin on cultured cells, its effect on terminally differentiated tissue in vivo has not been examined. Because of its highly organized structure, the retina was a model tissue with which to initiate such studies. Preliminary studies showed that the effects of lovastatin were qualitatively similar for intravitreal injections in the range of 0.05–0.25 μmol/eye. In contrast, no effects were observed below 0.05 μmol and panretinal necrosis was observed at doses ≥0.37 μmol (data not shown).

To identify the progression of morphologic changes in the rat retina, several postinjection time points were evaluated. Control eyes injected with Tris buffer (Fig. 2, *A* and *B*) displayed the typical retinal cytoarchitecture and stratification as observed in untreated animals. Fig. 2, *C–F* shows morphologic changes near the site of drug deposition at 1–2 d after injection. A gradient of effect was observed with the area near the site of injection most disrupted, and more peripheral areas less affected. Peripheral areas away from the site of injection were unaffected (not shown). At 1 d after injection of lovastatin (Fig. 2, *C* and *D*), the onl and olm took on a wavy appearance and pho-

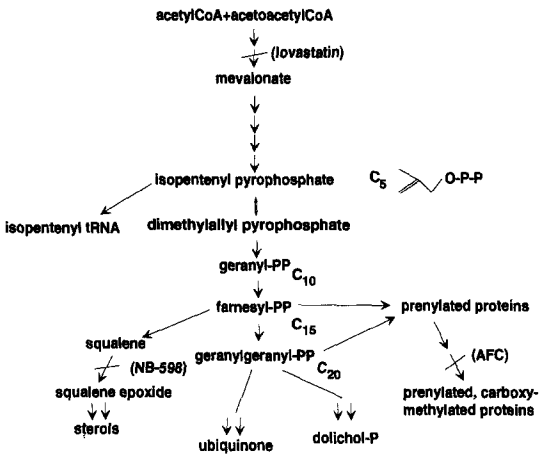

Figure 1. The mevalonate pathway. Mevalonate (derived from acetylCoA) is converted in several steps (indicated by arrows) to a five carbon isoprene unit, which is the precursor to all products of the various branches of the pathway. The enzymatic steps inhibited by lovastatin, NB-598, and AFC are shown. Side by side arrows indicate multiple steps required that are not shown in detail.

toreceptor nuclei were displaced from their usual position. Rod outer segments were intact, but were misaligned. Vacuoles were observed in and around the inl and gcl. At 2 d after injection, focal invaginations were observed in the onl, consistent with the early stages of rosette formation (Fig. 2, *E* and *F*). There was also evidence of ris and ros degeneration (i.e., truncation and misalignment). The distal ends of the outer segments became oriented towards the center of the newly forming rosettes. Rosettes comprised of photoreceptor nuclei were clearly distinguishable at 6 d after lovastatin treatment (Fig. 3 *A*). With the exception of compensatory displacement of inl cells, the rpe and other retinal cells appeared relatively unaffected. Rosette structure was seen as a circular arrangement of photoreceptor cell nuclei in layers of 2–6 cells in thickness (Fig. 3 *B*). Macrophages were typically seen in and around the rosettes. By 21 d after injection, photoreceptor nuclei had assumed a more random distribution throughout the affected region (Fig. 3, *C* and *D*). Despite these dramatic changes in retinal organization, a surprising number of photoreceptor nuclei persisted and no pyknotic nuclei were observed in any of the retinal layers. Rod inner and outer segments were not detectable at the light microscopic level. Retinal vessels showed numerous lumina, indicating that capillary shunting had occurred. Migration of rpe-like pigment granule containing cells into the outer retina and around blood vessels in the inner retina was also apparent at the later timepoint (Fig. 3 *D*) indicating possible rpe involvement.

To provide further insight into the nature of the lovastatin-induced disruption, electron microscopy was performed. Remnants of rod inner and outer segments were seen in the interior of rosettes at 6 d after injection (Fig. 4 *A*). By 21 d after injection, photoreceptor remnants were very sparse (Fig. 4 *B*). Small packets of rod outer segment disks were occasionally observed in close proximity to associated nuclei surrounded by minimal cytoplasm containing what appeared to be mitochondria and other organelles. These results indicate that lovastatin treatment is not simply leading to cell death, but rather appears to be affecting specific aspects of organelle integrity and retinal cytoarchitecture.

Persistence of Lovastatin Inhibitory Activity after Lovastatin Injection

We previously demonstrated short-term inhibition of the retina isoprenoid lipid biosynthetic pathway by lovastatin upon coinjection with [^{3}H]acetate in rats (Fliesler et al., 1993), however, we did not examine the persistence of this effect. To determine the persistence of lovastatin inhibition we evaluated [^{3}H]acetate incorporation in drug-injected and contralateral (control) eyes at 1 or 7 d. The corresponding radio-HPLC profiles of the retina nonsaponifiable lipids are shown in Fig. 5. In the control (Fig. 5 *A*), a prominent, symmetrical peak of radioactivity was coincident with the endogenous cholesterol mass (retention time, 10.8 min). In striking contrast, at both 1 (Fig. 5 *B*) and 7 d (Fig. 5 *C*) after a single lovastatin treatment, no incorporation of radioactivity into cholesterol was observed. In the latter two samples, the total incorporation of radioactivity into retina nonsaponifiable lipids was reduced by 93% and 99%, respectively, relative to the controls. Hence, a single intravitreal injection of lovastatin virtually abolished isoprenoid lipid biosynthesis, and the inhibitory action persisted for at least 7 d. Since HMG-CoA reductase (e.g., in rat liver) has a half-life of ~2–3 h (Dugan et al., 1972), these results further suggest that lovastatin itself persists in the eye at pharmacologically effective levels.

Inhibition of Sterol Synthesis Does Not Induce Histological Changes in the Retina

To examine the potential involvement of cholesterol deprivation in the lovastatin-induced pathology, NB-598, a selective inhibitor of squalene-2,3-epoxidase (Horie et al., 1990), was intravitreally injected into one eye, while the contralateral eye received Me_2SO alone. Morphological analysis was then performed at 3 and 7 d after injection (two animals per time point). We previously showed that 50 μg of NB-598 was effective in blocking conversion of coinjected [^{3}H]acetate to cholesterol in the rat retina, with resulting accumulation of radiolabeled squalene and squalene mass over a 6-h period (Fliesler et al., 1993). Examination of the retinas from NB-598–treated eyes revealed that their morphology was essentially identical to vehicle-injected controls (not shown). Therefore, either retinal requirements for cholesterol and other sterols are maintained by extra-ocular sources, or else a sufficient endogenous sterol pool exists in the retina to satisfy cholesterol requirements over the 1-wk observation period. However, these results do not rule out the possibility of recovery from NB-598 inhibition of sterol synthesis. To examine the persistence of squalene epoxidase inhibition by NB-598, rat eyes were injected with [^{3}H]acetate, 3 or 7 d after intravitreal injection with NB-598 (50 μg, in 5 μl of Me_2SO) or with Me_2SO alone. In the series shown, ~75–80% of the total nonsaponifiable radioactivity in controls (Fig. 6 *A*) comigrated with the endogenous cholesterol mass (retention time, 13.5 min). 3 d after administration of NB-598 (Fig. 6 *B*), ~80–85% of the total nonsaponifiable radioactivity was coincident with the elution position of squalene

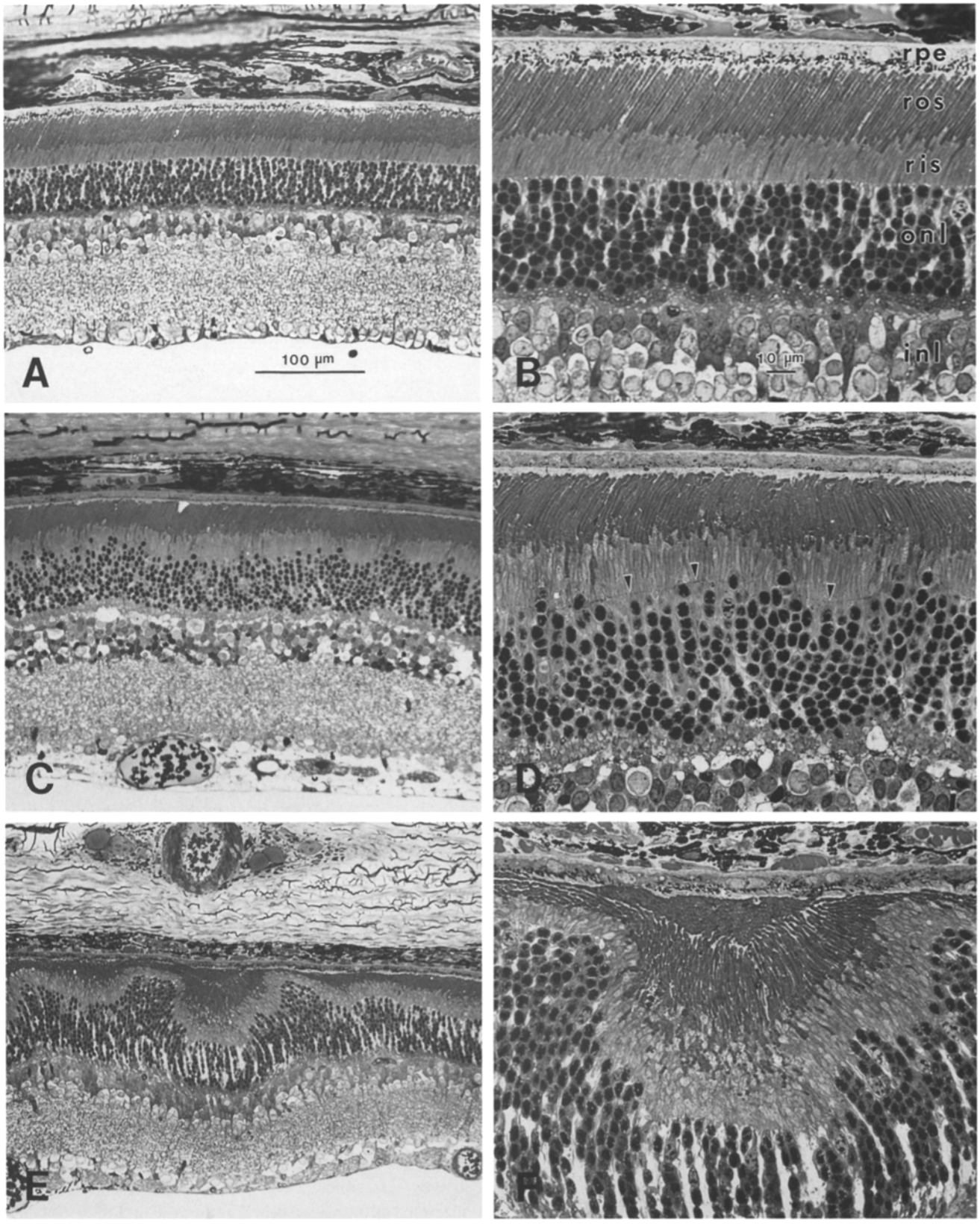

Figure 2. Early changes in the structural organization of the retina caused by intravitreal injection of 0.25 μmol lovastatin. (*A* and *B*) Control retina from eyes injected with Tris-HCl, pH 7.4; (*C* and *D*) retina 1 d after lovastatin injection; (*E* and *F*) retina 2 d after lovastatin injection. The micrographs on the right (*B*, *D*, and *F*) are higher magnifications of representative regions from the lower power micrographs on the left (*A*, *C*, and *E*). In *D*, the outer limiting membrane (*arrowheads*) follows the wave-like displacement of the outer nuclear layer at 1 d after injection. Abbreviations: *rpe*, retinal pigment epithelium; *ros*, rod outer segments; *ris*, rod inner segments; *onl*, outer nuclear layer; *inl*, inner nuclear layer. Bars: (*A*, *C*, and *E*) 100 μm; (*B*, *D*, and *F*) 1 μm, central inferior region.

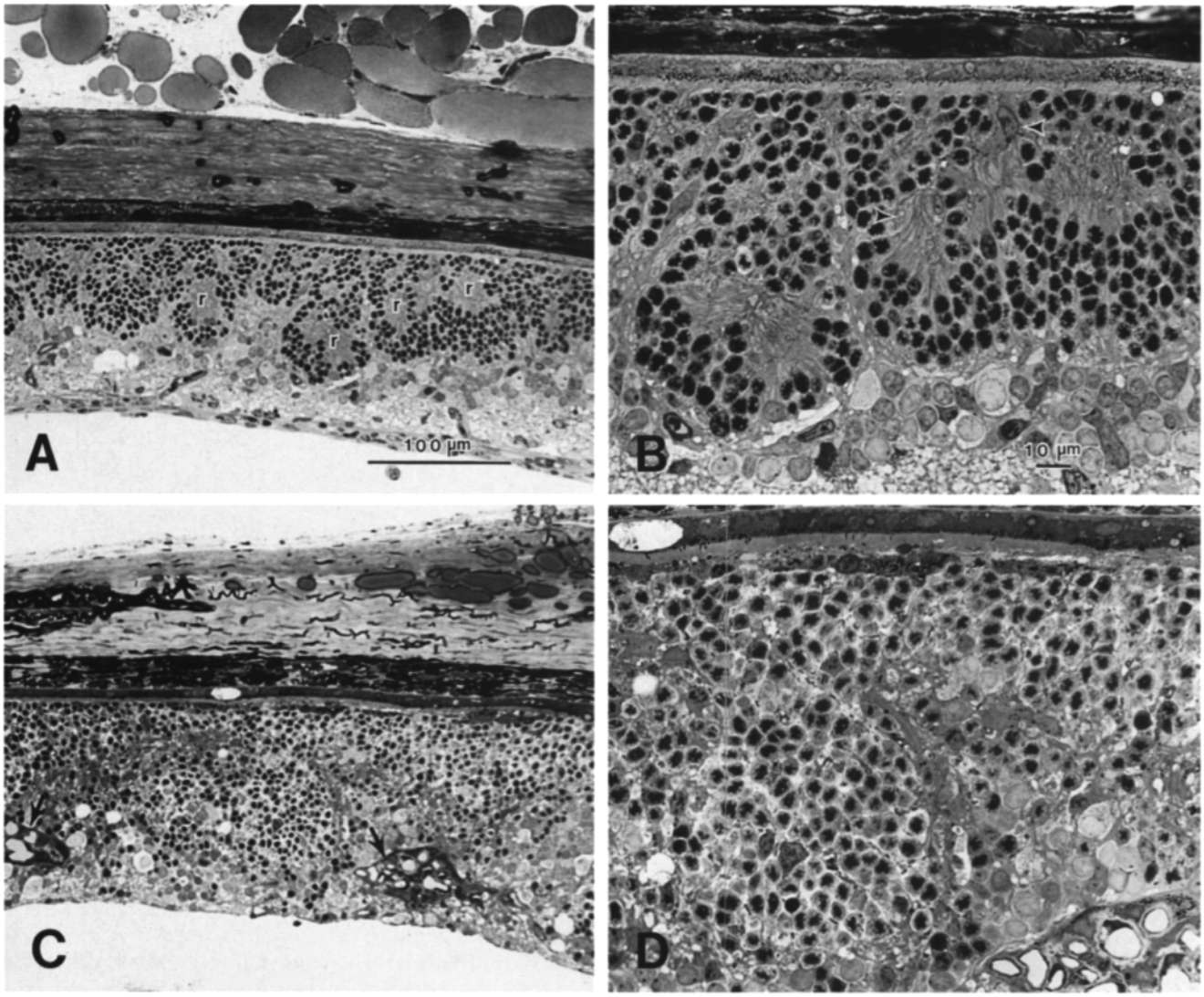

Figure 3. Changes in retinal structure at 6- (*A* and *B*) and 21-d (*C* and *D*) after intravitreal injection of 0.25 μmol lovastatin. Micrographs *B* and *D* are higher magnifications of *A* and *C*, respectively, as in Fig. 1. In *A*, photoreceptor nuclei have organized into rosettes (*r*) at 6 d after injection. In *B*, macrophages (*arrowheads*) are seen in the interior of the rosettes. Rosettes are not seen at 21 d after injection (*C* and *D*); instead, photoreceptor nuclei are scattered throughout the retina. Retinal vessels (*arrows*) take on an unusual appearance with numerous lumina, suggesting that capillary shunting has occurred. Bars: (*A* and *C*) 100 μm; (*B* and *D*) 1 μm, central inferior region.

(retention time, 15.5 min), whereas only ~4–5% of the radioactivity was coincident with cholesterol. In addition, whereas squalene mass is virtually undetectable in normal rat retinas (*cf.* Fig. 5, *A–C* and Fig. 6 *A*), significant accumulation of squalene mass was noted, to a level approaching 5–7 mol % of the cholesterol mass. At 7 d after injection with NB-598 (Fig. 6 *C*), radioactivity derived from [^{3}H]acetate was still largely accumulating as squalene, while cholesterol only accounted for ~10–12% of the total nonsaponifiable radioactivity. Also, the accumulation of squalene mass was even greater than at the 3-d time point (cholesterol:squalene mole ratio, ~4:1). Hence, although the inhibitory activity of NB-598 at the given dosage was not quantitative in this experiment, significant inhibition of squalene epoxidase persisted for at least 7 d after a single intravitreal injection of NB-598. Surprisingly, there was no appreciable decrease in total cholesterol mass of NB-598–treated retinas, compared with controls. In total, these findings indicate that inhibition of de novo cholesterol synthesis does not underlie the lovastatin-induced pathology.

Effects of Intravitreal AFC

A direct link between the observed, lovastatin-induced morphologic changes and inhibition of the function of prenylated proteins was suggested by subsequent results obtained by intravitreal injection of *N*-acetyl-*S-trans,trans*-farnesyl-L-cysteine (AFC). A dosage of 0.41 μmol dissolved in DMSO was grossly cytotoxic, producing panretinal necrosis with marked cell loss and gliotic scarring (not shown). Injection of 0.07–0.27 μmol produced morphological changes strikingly similar to those observed with lova-

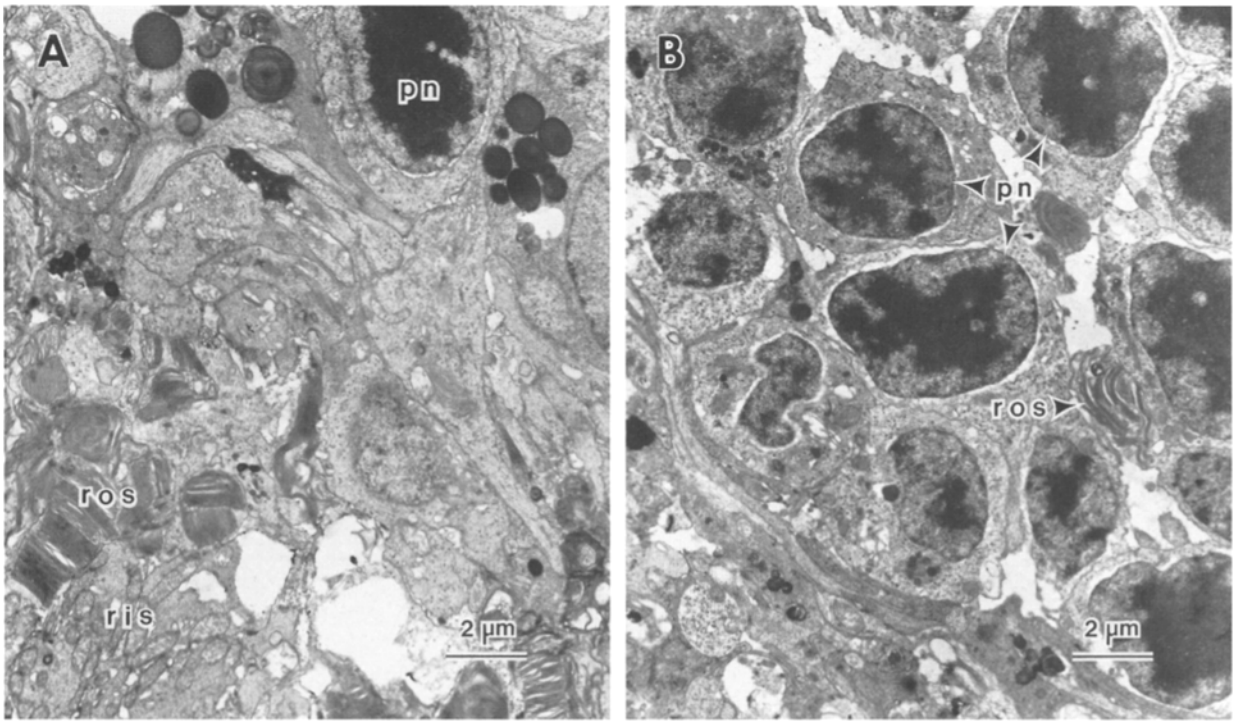

Figure 4. Electron micrographs 6 (*A*) and 21 d (*B*) after injection of 0.25 μmol lovastatin. In *A*, showing interior of rosette, rod outer segment fragments (*ros*) containing membranous disks, and portions of rod inner segments (*ris*) are clearly observed. One photoreceptor nuclei (*pn*) forming part of the rosette is also seen. In *B*, most photoreceptor nuclei (*pn*) are partially or completely surrounded by sparse cytoplasm with organelles. Severely truncated stacks of disorganized ros disks (*ros*) are occasionally seen. Bars: (*A*) 2 μm; (*B*) 2 μm.

statin, including rosette formation and migration of photoreceptor nuclei into other retinal layers (Fig. 7); in contrast, DMSO-injected controls displayed no pathology (not shown; cf. Fig. 2, *A* and *B*). Taken together, these results implicate alteration of prenylated protein function as the primary cause of the lovastatin- and AFC-induced morphological alterations.

Discussion

We have shown that in vivo inhibition of the mevalonate pathway leads to gross disruption of cytoarchitecture in the adult rat retina. This is the first study to demonstrate an effect of lovastatin in nondividing, terminally differentiated neural cells in vivo. This is an important distinction

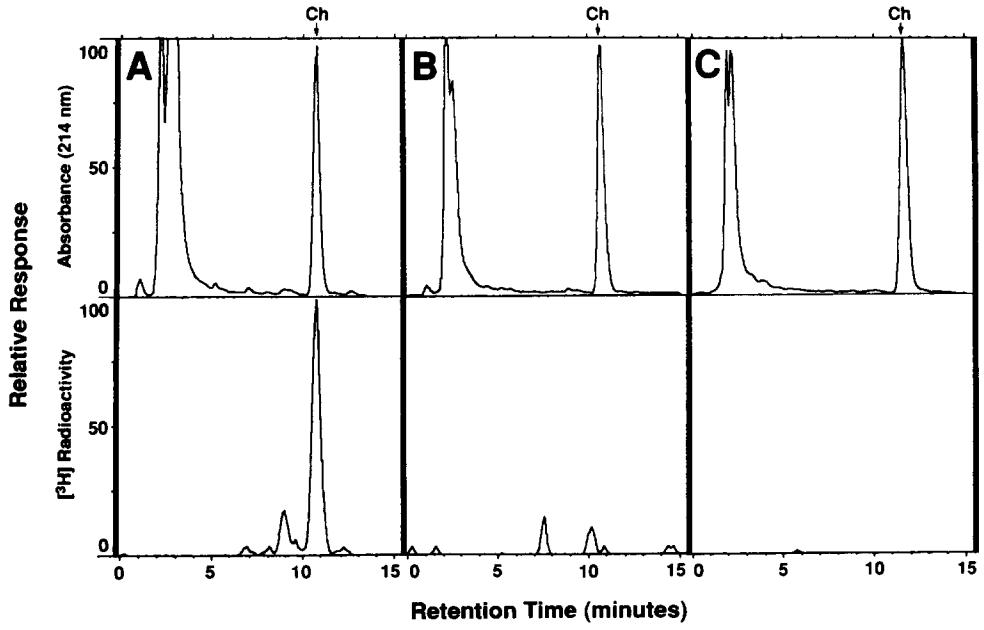

Figure 5. Persistence of the lovastatin effect. Reverse-phase HPLC radiochromatograms of control (*A*) and lovastatin-treated (*B* and *C*) rat retina nonsaponifiable lipids obtained 6 h after intravitreal injection with [^{3}H]acetate. Control eyes were injected with 5 μl buffer alone; treated eyes received lovastatin (100 μg in 5 μl buffer), 1 (*B*) or 7 (*C*) d before [^{3}H]acetate injection. (*Upper panels*) Endogenous mass detected by uv absorbance (214 nm), with relative scale adjusted so as to yield a full-scale absorbance for the cholesterol peak (retention time, 10.8 min); (*lower panels*) ^{3}H radioactivity (*A*, 74,100 dpm; *B*, 5,300 dpm; *C*, 200 dpm). The elution position of an authentic cholesterol standard (*Ch*) is indicated.

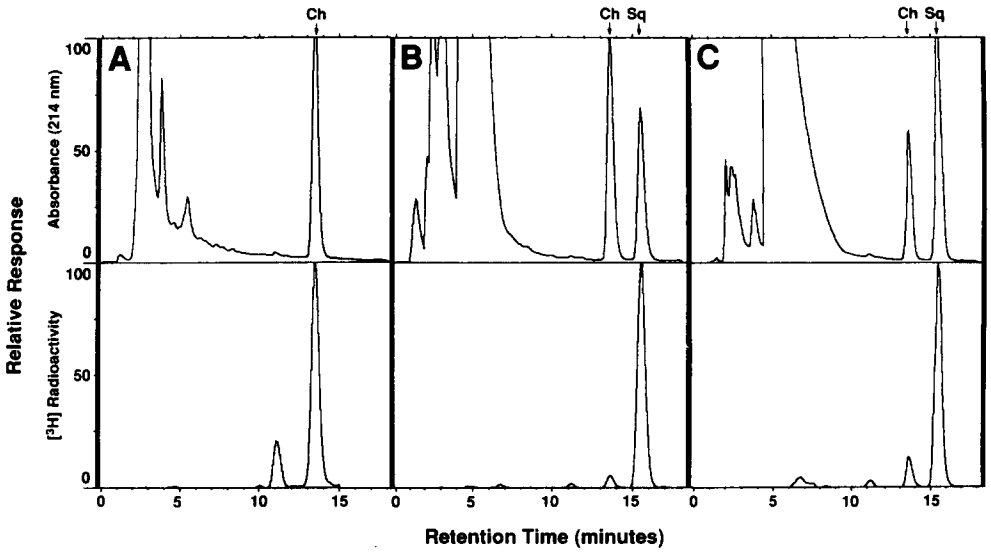

Figure 6. Persistence of NB-598 inhibition of sterol synthesis. Reverse-phase HPLC radiochromatograms of nonsaponifiable lipids from control (*A*) and NB-598–treated (*B* and *C*) rat retinas obtained 6 h after intravitreal injection with [^{3}H]acetate. Control eyes were injected with 5 μl of Me_2SO alone; treated eyes received NB-598 (50 μg in 5 μl of Me_2SO), 3 (*B*) or 7 (*C*) d before [^{3}H]acetate injection. (*Upper panels*) Endogenous mass detected by uv absorbance (214 nm), with relative scale adjusted so as to yield a full-scale absorbance for the cholesterol peak (retention time, 13.5 min); (*lower panels*) ^{3}H radioactivity, with relative scale adjusted so as to yield a full-scale response for the peak corresponding to cholesterol (*total radioactivity*: *A*, 106,300 dpm; *B*, 209,200 dpm; *C*, 94,800 dpm). The elution positions of authentic standards of cholesterol (*Ch*) and squalene (*Sq*) are indicated by the arrows.

from studies with lovastatin in cell culture, because the effects of lovastatin can be observed independent of pathways involved in cell division where the functions of several prenylated proteins are critical (e.g., *ras*, lamins A and B). The primary effect of lovastatin in the adult retina appears to involve the photoreceptor layer and outer limiting membrane (Fig. 2, *C* and *D*). Over the time course of lovastatin-induced alterations, there was nearly complete degeneration of the photoreceptor inner and outer segments. However, the photoreceptor cells apparently did not die, since their nuclei and some other organelles remained intact (Fig. 4 *B*). Even at timepoints as long as three months after a single injection, qualitative observation indicated virtually no change in the relative numbers of intact photoreceptor nuclei from that observed at 21 d. Within 6 d after injection, the photoreceptor nuclei migrated from their usual position in the outer nuclear layer and formed rosettes similar to those observed in retinal dysplasia in humans (Duke-Elder, 1963) and other animals (Chader et al., 1988; Whitely, 1991). To our knowledge, drug-induced dysplastic-like changes in a fully differentiated adult retina have not been reported, however, their possible natural occurrence in the human retina has been observed (Lahav et al., 1975). The relationship, if any, between rosettes occurring as developmental anomalies and those induced by lovastatin remains to be determined.

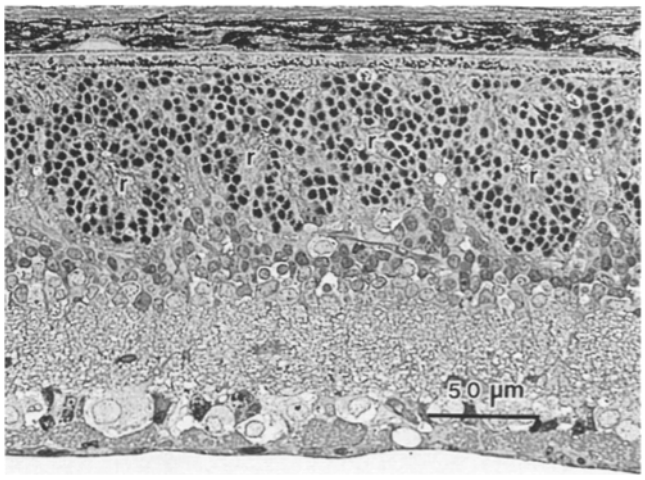

Figure 7. Retinal changes 4 d after intravitreal injection of 50 μg AFC. Photoreceptor rosettes (*r*) are essentially identical to those observed 6 d after intravitreal injection of lovastatin (cf. Fig. 3 *A*). Bar, 250 μm.

The observed histological disruption induced by intravitreal lovastatin could have been due to inhibition of any of the branchpoints of the mevalonate pathway as shown in Fig. 1. The results reported here coupled with those of previous studies allow one to rule out the involvement of all branchpoints except the posttranslational processing of proteins by prenylation. Previous studies employing intravitreally injected tunicamycin (Fliesler et al., 1984), an inhibitor of dolichol-dependent protein glycosylation, demonstrated a degenerative effect that is markedly different from that obtained with lovastatin. Under suitable conditions, intravitreal tunicamycin injection in adult animals leads to a photoreceptor-specific degeneration that does not result in rosette formation or disruption of retinal stratification. Hence, it is unlikely that the lovastatin-induced degenerative changes are a consequence of perturbation of dolichylphosphate pools (a significant reduction of which might result in inhibition of protein glycosylation).

Cholesterol is a significant constituent of the plasma membrane of most eukaryotic cells, although in photoreceptor disk membranes cholesterol represents <10 mol % of the total membrane lipid (Fliesler and Anderson, 1983). However, cholesterol appears to be enriched in inner retinal cell layers, especially in the collective axonal processes (for a discussion, see Fliesler and Anderson, 1983). Thus, we evaluated whether or not inhibition of sterol synthesis

was responsible for the observed histological changes induced by lovastatin. Intravitreal injection of NB-598 specifically inhibited sterol synthesis (Fig. 6) without producing any alteration of retinal morphology. This finding suggests a lack of any significant contribution of de novo sterol synthesis disruption in the observed pathological changes induced by lovastatin. These results, taken together with those discussed above, and by a process of elimination (see Pittler et al., 1992), previously led us to speculate upon an involvement of prenylated proteins in the maintenance of retinal cytoarchitecture.

This presumed involvement of prenylated proteins was given further credence by results obtained with intravitreal injection of AFC. AFC is a potent competitive inhibitor of carboxymethylation of prenylated proteins (Volker et al., 1991), the only step in −CAAX processing that is reversible (Parish and Rando, 1994). The effects of AFC were strikingly similar to those observed with lovastatin (cf. Fig. 3 *A* and Fig. 7), indicating a requirement of one or more prenylated/carboxymethylated proteins in the maintenance of adult retinal cytoarchitecture. A functional role for prenylated protein carboxymethylation has been suggested for visual transduction in ros (Pérez-Sala et al., 1991; Ohguro et al., 1991; Parish and Rando, 1994), for modulation of insulin secretion in islet cells (Metz et al., 1993), for agonist–receptor-mediated signal transduction in platelets (Akbar et al., 1993), for fMLP-induced signal transduction in neutrophils (Philips et al., 1993), and for efficient membrane binding and function of the small GTP-binding protein ras (Hancock et al., 1991). While it is clear that AFC does inhibit the carboxymethyltransferase in vitro, its mechanism of action in vivo is less certain. AFC was shown to inhibit chemotaxis of macrophages in a manner inconsistent with inhibition of carboxymethylation (Scheer and Gierschik, 1993). Using a series of farnesylcysteine derivatives it was shown that analogues that do not inhibit the methyltransferase can still block superoxide release in neutrophils (Ding et al., 1994) and platelet aggregation (Ma et al., 1994). It was suggested that AFC may act to alter heterotrimeric G-protein βγ function (Ding et al., 1994), perhaps by interfering with protein–protein interactions requiring a carboxymethylated prenylcysteine. While the exact mechanism of action of AFC remains to be established, it is accepted that AFC affects the function of prenylated protein, and thus our results with AFC support the participation of prenylated protein in the maintenance of adult retinal structure.

Protein prenylation is a permanent covalent modification that occurs immediately after polypeptide synthesis (Goldstein and Brown, 1990; Rando, 1992). Thus, only prenylated proteins that turn over in less than 24 h are likely to be candidates for producing the lovastatin-induced changes within the observed time course. Therefore, we propose that one or more of the several previously identified prenylated proteins in adult rat retina (Anant et al., 1992) are involved in the lovastatin/AFC-induced effects. Four of these proteins are photoreceptor specific (cGMP phosphodiesterase α and β subunits, transducin γ subunit, rhodopsin kinase) and function in phototransduction, and at least three are small, *ras*-like GTP-binding proteins. A null mutation in the rod cGMP phosphodiesterase β subunit in mice (Pittler and Baehr, 1991) or dogs (Suber et al., 1993) leads to photoreceptor degeneration, but does not mimic the lovastatin effect. Defects in other photoreceptor specific proteins, including rhodopsin and peripherin/*rds*, which are both integral membrane proteins, also lead to photoreceptor degeneration (Humphries et al., 1992; Kajiwara et al., 1992), without initially effecting other retinal cell types or forming rosettes. It is expected that the effects of mutations in rhodopsin kinase or transducin γ-subunit are also unlikely to mimic the morphologic effects induced by lovastatin. It cannot be ruled out that inhibition of function of quantitatively minor or unknown prenylated proteins is responsible for the lovastatin- and AFC-induced morphologic changes; however, we consider the small GTP-binding proteins to be the most likely candidates in the etiology of the induced degeneration.

Several reports have now clearly shown a role for the small GTP-binding proteins of the *rho* class in the modulation of the actin cytoskeleton (for review see Nobes and Hall, 1994; also see the Introduction). A functional role for small GTP-binding proteins in phototransduction has also been suggested in squid and bovine photoreceptors (Wieland et al., 1990; Petrov et al., 1994) and *Limulus* photoreceptors (Stieve et al., 1992). Small GTP-binding proteins of the *rab* family are critical for the intracellular transport of rhodopsin-containing vesicles (Deretic and Papermaster, 1993). Since lovastatin and AFC could inhibit the function of several different GTP-binding proteins (as well as several other prenylated proteins) in many diverse pathways, it is likely that the observed effects are pleiotropic. The loss of outer segments could be due to inhibition of *rabs* required for vesicle transport of rhodopsin, an important structural component of disk membranes (Sung et al., 1991), while the loss of stratification could be due to inhibition of *rho* function required for proper microfilament organization. Nonetheless, our results are the first to draw attention to the structural role of prenylated proteins in promoting and maintaining normal retinal cytoarchitecture.

The morphological changes observed upon intravitreal injection of lovastatin or AFC are consistent with the model for maintenance of retinal cytoarchitecture as proposed by Madreperla and Adler (1989). In this model, opposing forces provided by microtubule and microfilament networks function to maintain retinal structural integrity. If one force component is severed or greatly reduced in numbers (i.e., microfilament arrays), as we propose may be the case in the lovastatin and AFC treatments, then a dramatic movement of cells might result, due to the continuing unopposed force provided by the other component. The early time points of lovastatin treatment indicate gross movements of cells (see Fig. 2, *C–F*) that may be occurring as microfilament networks (with their associated tensile strengths) dissolve. Over time and due to the persistence of lovastatin, more and more of the microfilament arrays break down with eventual complete loss of retinal cytoarchitecture (Fig. 3, *C–D*). We are currently focusing on identifying the prenylated proteins that are presumed responsible for the observed lovastatin and AFC-induced pathologic effects, and on evaluating which cytoskeletal elements are affected.

We thank Richard Florman and Luanne Oliveira for expert technical assistance, and Dr. David Saperstein for assistance with some of the intravit-

real injections. We also thank Dr. Ronald Balczon for critical comments on the manuscript.

This work was supported in part by the National Science Foundation IBN 911332, The Eppley Foundation for Research, Inc., and the American Heart Association, Alabama Affiliate to S. J. Pittler; EY07361 to R. K. Keller and S. J. Fliesler; EY04554 to L. M. Rapp and unrestricted Departmental grants from Research to Prevent Blindness, Inc. to Baylor College of Medicine, Department of Ophthalmology (L. M. Rapp) and to Anheuser-Busch Eye Institute, Saint Louis University (S. J. Fliesler). S. J. Fliesler is a Research to Prevent Blindness James S. Adams Scholar.

Received for publication 13 January 1995 and in revised form 18 April 1995.

References

Akbar, H., W. Wang, R. Kornhauser, C. Volker, and J. B. Stock. 1993. Protein prenylcysteine analog inhibits agonist-receptor-mediated signal transduction in human platelets. *Proc. Natl. Acad. Sci. USA.* 90:868–872.

Anant, J. S., O. C. Ong, H. Xie, S. Clarke, P. J. O'Brien, and B. K.-K. Fung. 1992. *In vivo* differential prenylation of retinal cyclic GMP phosphodiesterase catalytic subunits. *J. Biol Chem.* 267:687–690.

Chader, G. J., G. Aguirre, and S. Sanyal. 1988. Studies on animal models of retinal degeneration. *In* Retinal Diseases: Biomedical Foundations and Clinical Management. M. O. M. Tso, editor. J. B. Lipincott Co., Philadelphia, PA. 80–89.

Deretic, D., and D. S. Papermaster. 1993. Rab6 is associated with a compartment that transports rhodopsin from the *trans*-Golgi to the site of rod outer segment disk formation in frog retinal photoreceptors. *J. Cell Sci.* 106:803–813.

Ding, J., D. J. Lu, D. Pérez-Sala, Y. T. Ma, J. F. Maddox, B. A. Gilbert, J. A. Badwey, and R. R. Rando. 1994. Farnesyl-L-cysteine analogs can inhibit or initiate superoxide release by human neutrophils. *J. Biol. Chem.* 269:16837–16844.

Dugan, R. E., L. L. Slakey, A. V. Bridis, and J. W. Porter. 1972. Factors affecting the diurnal variation in the level of β-hydroxy-β-methylglutaryl coenzyme A reductase and cholesterol-synthesizing activity in rat liver. *Arch. Biochem. Biophys.* 152:21–27.

Duke-Elder, S. 1963. Congenital deformities. *In* System of Ophthalmology. Vol. III. part II. Stewart Duke-Elder, editor. The CV Mosby Co., St. Louis, MO. 628–634.

Fenton, R. G., H. Kung, D. L. Longo, and M. R. Smith. 1992. Regulation of intracellular actin polymerization by prenylated cellular proteins. *J. Cell Biol.* 117:347–356.

Fliesler, S. J., and R. E. Anderson. 1983. Chemistry and metabolism of lipids in the vertebrate retina. *Prog. Lipid. Res.* 22:79–131.

Fliesler, S. J., L. M. Rapp, and J. G. Hollyfield. 1984. Photoreceptor-specific degeneration caused by tunicamycin. *Nature (Lond.).* 311:575–577.

Fliesler, S. J., R. Florman, L. M. Rapp, S. J. Pittler, and R. K. Keller. 1993. In vivo biosynthesis of cholesterol in the rat retina. *FEBS (Fed. Eur. Biochem. Soc.) Lett.* 335:234–238.

Fukada, Y., T. Takao, H. Ohguro, T. Yoshizawa, T. Akino, and Y. Shimonishi. 1990. Farnesylated γ-subunit of photoreceptor G protein indispensable for GTP-binding. *Nature (Lond.).* 346:658–660.

Goldstein, J. L., and M. S. Brown. 1990. Regulation of the mevalonate pathway. *Nature (Lond.).* 343:425–430.

Hall, A. 1993. Ras-related proteins. *Curr. Opin. Cell Biol.* 5:265–268.

Hancock, J. F., K. Cadwallader, and C. J. Marshall. 1991. Methylation and proteolysis are essential for efficient membrane binding of prenylated p21K-ras(B). *EMBO (Eur. Mol. Biol. Organ.) J.* 10:641–646.

Horie, M., Y. Tsuchiya, M. Hayashi, Y. Iida, Y. Iwasawa, Y. Nagata, Y. Sawasaki, H. Fukuzumi, K. Kitani, and T. Kamei. 1990. NB-598: a potent competitive inhibitor of squalene epoxidase. *J. Biol. Chem.* 265:18075–18078.

Humphries, P., P. Kenna, and G. J. Farrar. 1992. On the molecular genetics of retinitis pigmentosa. *Science (Wash. DC).* 256:804–808.

Inglese, J., J. F. Glickman, W. Lorenz, M. G. Caron, and R. J. Lefkowitz. 1992. Isoprenylation of a protein kinase. Requirement of farnesylation/α-carboxyl methylation for full enzymatic activity of rhodopsin kinase. *J. Biol. Chem.* 267:1422–1425.

Jalink, K., E. J. Van Corven, T. Hengeveld, N. Morii, S. Narumiya, and W. H. Moolenaar. 1994. Inhibition of lysophosphatidate- and thrombin-induced neurite retraction and neuronal cell rounding by ADP ribosylation of the small GTP-binding protein Rho. *J. Cell Biol.* 126:801–810.

Kajiwara, K., L. B. Hahn, S. Mukai, G. H. Travis, E. L. Berson, and T. P. Dryja. 1991. Mutations in the human retinal degeneration slow gene in autosomal dominant retinitis pigmentosa. *Nature (Lond.).* 354:480–483.

Keller, R. K., S. J. Fliesler, and S. W. Nellis. 1988. Isoprenoid biosynthesis in the retina. *J. Biol. Chem.* 263:2250–2254.

Kita, T., M. S. Brown, and J. L. Goldstein. 1980. Feedback regulation of 3-hydroxy-3-methylglutaryl coenzyme A reductase in livers of mice treated with mevinolin, a competitive inhibitor of the reductase. *J. Clin. Invest.* 66: 1094–1100.

Lahav, M., D. M. Albert, and J. L. Craft. 1975. Light and electron microscopic study of dysplastic rosette-like structures occurring in the disorganized mature retina. *Albrecht v. Graefes Arch. Klin. Exp. Ophthal.* 195:57–68.

Ma, Y.-T., Y.-Q. Shi, Y. H. Lim, S. H. McGrail, J. A. Ware, and R. R. Rando. 1994. Mechanistic studies on human platelet isoprenylated protein methyltransferase: farnesylcysteine analogs block platelet aggregation without inhibiting the methyltransferase. *Biochemistry.* 33:5414–5420.

Madreperla, S. A., and R. Adler. 1989. Opposing microtubule- and actin-dependent forces in the development and maintenance of structural polarity in retinal photoreceptors. *Dev. Biol.* 131:149–160.

Maltese, W. A. 1990. Posttranslational modification of proteins by isoprenoids in mammalian cells. *FASEB (Fed. Am. Soc. Exp. Biol.) J.* 4:3319–3328.

Metz, S. A., M. E. Rabaglia, J. B. Stock, and A. Kowluru. 1993. Modulation of insulin secretion from normal rat islets by inhibitors of the post-translational modifications of GTP-binding proteins. *Biochem. J.* 295:31–40.

Nobes, C., and A. Hall. 1994. Regulation and function of the Rho subfamily of small GTPases. *Curr. Opin. Genet. Dev.* 4:77–81.

Norman, J. C., L. S. Price, A. J. Ridley, A. Hall, and A. Koffer. 1994. Actin filament organization in activated mast cells is regulated by heterotrimeric and small GTP-binding proteins. *J. Cell Biol.* 126:1005–1016.

Ohguro, H., Y. Fukada, T. Takao, Y. Shimonishi, T. Yoshizawa, and T. Akino. 1991. Carboxyl methylation and farnesylation of transducin gamma-subunit synergistically enhance its coupling with metarhodopsin II. *EMBO (Eur. Mol. Biol. Organ.) J.* 10:3669–3674.

Parish, C. A., and R. R. Rando. 1994. Functional significance of G protein carboxymethylation. *Biochemistry.* 33:9986–9991.

Paterson, H. F., A. J. Self, M. D. Garrett, I. Just, K. Aktories, and A. Hall. 1990. Microinjection of recombinant $p21^{rho}$ induces rapid changes in cell morphology. *J. Cell Biol.* 111:1001–1007.

Pérez-Sala, D., E. W. Tan, F. J. Canada, and R. J. Rando. 1991. Methylation and demethylation reactions of guanine nucleotide-binding proteins of retinal rod outer segments. *Proc. Natl. Acad. Sci. USA.* 88:3043–3046.

Petrov, V. M., I. D. Artamonov, and V. M. Lipkin. 1994. Small GTP-binding proteins of squid photoreceptor: interaction with photoactivated rhodopsin. *FEBS (Fed. Eur. Biochem. Soc.) Lett.* 337:274–276.

Philips, M. R., M. H. Pillinger, R. Staud, C. Volker, M. G. Rosenfeld, G. Weissmann, and J. B. Stock. 1993. Carboxyl methylation of Ras-related proteins during signal transduction in neutrophils. *Science (Wash. DC).* 259:977–980.

Pittler, S. J., and W. Baehr. 1991. Identification of a nonsense mutation in the rod photoreceptor cGMP PDE β-subunit gene of the *rd* mouse. *Proc. Natl. Acad. Sci. USA.* 88:8322–8326.

Pittler, S. J., S. J. Fliesler, and L. M. Rapp. 1992. Novel morphological changes in rat retinas induced by intravitreal lovastatin. *Exp. Eye Res.* 54:149–152.

Qin, N., S. J. Pittler, and W. Baehr. 1992. *In vitro* isoprenylation, and membrane association of mouse rod photoreceptor cGMP phosphodiesterase α and β subunits expressed in bacteria. *J. Biol. Chem.* 267:8458–8463.

Rando, R. R. 1992. Postranslational modifications of retinal G proteins. *Struct. Funct. Retinal Prot.* 221:365–368.

Rapp, L. M., and S. C. Smith. 1992. Morphological comparisons between rhodopsin-mediated and short-wavelength classes of retinal light damage. *Invest. Ophthalmol. Vis. Sci.* 33:3367–3377.

Ridley, A. J., and A. Hall. 1992. The small GTP-binding protein rho regulates the assembly of focal adhesions and actin stress fibers in response to growth factors. *Cell.* 70:389–399.

Ridley, A. J., H. F. Paterson, C. L. Johnston, D. Keikmann, and A. Hall. 1992. The small GTP-binding protein rac regulates growth factor-induced membrane ruffling. *Cell.* 70:401–410.

Scheer, A., and P. Gierschik. 1993. Farnesylcysteine analogues inhibit chemotactic peptide receptor-mediated G-protein activation in human HL-60 granulocyte membranes. *FEBS (Fed. Exp. Biochem. Soc.) Lett.* 319:110–114.

Schroepfer, G. J. Jr. 1981. Sterol biosynthesis. *Annu. Rev. Biochem.* 50:585–621.

Sinensky, M., and R. J. Lutz. 1992. The prenylation of proteins. *BioEssays.* 14: 25–31.

Stieve, H., B. Niemeyer, K. Aktories, and H. E. Hamm. 1992. Disturbing GTP-binding protein function through microinjection into the visual cell of *Limulus. Z. Naturforsch.* 47c:915–921.

Suber, M. L., S. J. Pittler, N. Qin, G. C. Wright, V. Holcombe, R. H. Lee, C. M. Craft, R. N. Lolley, W. Baehr, and R. L. Hurwitz. 1993. Irish setter dogs affected with rod/cone dysplasia contain a nonsense mutation in the rod cGMP phosphodiesterase β-subunit gene. *Proc. Natl. Acad. Sci. USA.* 90:3968–3972.

Sung, C.-H., B. G. Schneider, N. Agarwal, D. S. Papermaster, and J. Nathans. 1991. Functional heterogeneity of mutant rhodopsins responsible for autosomal dominant retinitis pigmentosa. *Proc. Natl. Acad. Sci. USA.* 88:8840–8844.

U.S. Department of Health and Human Services. 1985. Guide for the Care and Use of Laboratory Animals. NIH Publication No. 85–23.

Volker, C., R. A. Miller, W. R. McCleary, A. Rao, M. Poenie, J. M. Backer, and J. B. Stock. 1991. Effects of farnesylcysteine analogs on protein carboxyl methylation and signal transduction. *J. Biol. Chem.* 266:21515–21522.

Whitely, H. E. 1991. Dysplastic canine retinal morphogenesis. *Invest. Ophthalmol. Vis. Sci.* 32:1492–1497.

Wieland, T., I. Ulibarri, P. Gierschik, A. Hall, K. Aktories, and K. H. Jakobs. 1990. Interaction of recombinant rho A GTP-binding proteins with photoexcited rhodopsin. *FEBS (Fed. Exp. Biochem. Soc.) Lett.* 274:111–114.